Integrated Communication and Computing in Time-Varying mmWave Channels

Joan Çollaku*, Kuranage Roche Rayan Ranasinghe*, Niclas Führling*,
Giuseppe Thadeu Freitas de Abreu* and Takumi Takahashi†

*School of Computer Science and Engineering, Constructor University, Bremen, Germany
†Graduate School of Engineering, Osaka University, Suita, Japan
Emails: [jcollaku, kranasinghe, nfuehrling, gabreu]@constructor.university, takahashi@comm.eng.osaka-u.ac.jp

***Abstract*—We propose a novel framework for integrated communication and computing (ICC) transceiver design in time-varying millimeter-wave (mmWave) channels. In particular, in order to cope with the dynamics of time-varying mmWave channels, the detection of communication symbols and the execution of an over-the-air computing (AirComp) operation are performed in parallel with channel tracking, as opposed to existing state-of-the-art (SotA) on ICC where perfect knowledge of the channel at all time instances is typically assumed. For clarity of exposition, we consider a single-input multiple-output (SIMO) uplink scenario where multiple single-antenna user equipment (UE) transmit to a base station (BS) equipped with multiple antennas, such that each UE, or edge device (ED), precodes its own transmit signal, while the BS, or access points (APs), also performs receive beamforming. The proposed transceiver framework then estimates channel state information (CSI) and data symbols in parallel, using a bilinear Gaussian belief propagation (BiGaBP) algorithm for joint channel and data detection (JCDE), aided by a channel prediction (CP) algorithm executed before each estimation window at the BS. The AirComp operation is then executed by means of an optimal combination of the residual signal. Simulation results demonstrate the effectiveness of the proposed scheme in performing ICC in challenging time-varying mmWave channels, with minimal degradation to both communication and computing performance.**

***Index Terms*—Integrated communication and computing, bilinear Gaussian belief propagation, over-the-air computing, millimeter-wave channels, channel tracking**

I. Introduction

Due to the unrelenting demand for higher data rates and support for an increasingly large number of distinct applications, there is a need for the integration of new functionalities into communication systems. A prominent example is integrated sensing and communication (ISAC), which has gained much attention in recent years [1]–[4]; and another is the utilization of the properties of wireless channels to perform over-the-air computing (AirComp) [5]. In recognition to this opportunity, multiple works have proposed AirComp schemes [6]–[10], more recently giving rise to the notion of integrated communication and computing (ICC).

The above works assume, however, perfect knowledge of the channel, which is also a typical assumption made in the design of transceivers for millimeter-wave (mmWave) technology. Indeed, mmWave is a key approach to achieve higher rates in future wireless systems [11], [12], but effective beamforming [13]–[15] techniques required to mitigate the high propagation losses and blockage in mmWave channels also typically require perfect channel state information (CSI). Aiming at circumventing this challenge, work has been done to design receivers capable of performing either channel prediction (CP) CSI, or channel tracking, concomitant with the detection of communication symbols. Among various alternatives, the approach based on bilinear Gaussian belief propagation (BiGaBP) [16]–[19] has proved particularly advantageous, due to its excellent trade-off between performance and complexity.

In contribution to both these trends – of multi-functionality and resilience to time-varying behavior – we present in this article on a new BiGaBP-based framework to perform joint communication, computing and channel tracking (JCCCT) over a time-varying mmWave channels. Receivers designed under the BiGaBP framework have been previously employed for joint channel estimation and data detection [19], [20] in multiple-input multiple-output (MIMO) systems, while a linear Gaussian belief propagation (GaBP) receiver has been used for ICC in [10]. Our work follows on these footsteps, integrating to a BiGaBP joint channel and data detection (JCDE) receiver AirComp functionality via a minimum mean squared error (MMSE) combiner operated over the residual signal [10], [21].

The communication and computing signals are transmitted simultaneously by the user equipments (UEs)/edge devices (EDs) to be received at the base station (BS)/access point (AP), which performs receive beamforming and detection[1]. We assume that the channel in our first transmission time instance is known, and the time variation is tracked; then, the BiGaBP and CP algorithms described in [20] are used to estimate the communication symbols and the channel in parallel, while treating the superimposed computing signal as effective noise. The BiGaBP algorithm performs data estimation by passing messages on a tripartite graph, assuming Gaussian density functions for the interference and noise term in each received signal/channel coefficient, while the CP algorithm uses a Kalman filter-like mechanism to provide reliable estimates for the next window of JCDE.

It should be noted that while the JCDE & CP algorithm is the same one used in [20], this work contributes to the SotA by presenting a novel system template that integrates the functionality of AirComp into a high-mobility setting, which has the potential to become an important part of

[1]Throughout the article the terms UE and BS will be used interchangeably with ED and AP, respectively.

V2X communications. Additionally, the proposed framework enables AirComp in mmWave channels. The proposed system framework can then be used for ICC in the mmWave band in high-mobility communication scenarios, without having to continually transmit pilot symbols. Given this framework, further extensions such as multi-stream computation, or the computation of a wider range of nomographic functions also become possible under the same channel conditions.The integration of the AirComp operation into the JCDE procedure, which is currently performed disjointly from the JCDE phase, is also a further avenue to explore in future work.

In this work, we summarize the system model, describe the transmit signal and receiver design, and then evaluate the performance of the scheme in terms of communications bit error rate (BER) and normalized mean squared error (NMSE) for channel estimation and AirComp.

Notation: The following notation is used persistently in the manuscript. Vectors and matrices are represented by lowercase and uppercase boldface letters, respectively; $\mathbf{I}_M$ denotes an identity matrix of size M and $\mathbf{1}_M$ denotes a column vector composed of M ones; the Euclidean norm and the absolute value of a scalar are respectively given by $\|\cdot\|_2$ and $|\cdot|$; the transpose and hermitian operations follow the conventional form $(\cdot)^{\mathsf{T}}$ and $(\cdot)^{\mathsf{H}}$, respectively; $\Re\{\cdot\}$, $\Im\{\cdot\}$ and $\min(\cdot)$ represents the real part, imaginary part and the minimum operator, respectively. Finally, $\sim \mathcal{N}(\mu, \sigma^2)$ and $\sim \mathcal{CN}(\mu, \sigma^2)$ respectively denotes the Gaussian and complex Gaussian distribution with mean μ and variance σ^2, where $\sim$ denotes "is distributed as".

II. System Model

A. Channel Model

Consider a multi-user single-input multiple-output (SIMO) system with M single antenna UEs/EDs and a BS/AP with N_{RX} antennas, which employs receive beamforming as illustrated in Figure 1. Following existing literature [22]–[25], the channel is modeled using the mmWave cluster channel model, with L clusters having C_l rays each, where $l \in \{1, 2, \cdots, L\}$. The channel from the m-th UE/ED to the BS at a time instance k can be expressed as

$$\acute{\boldsymbol{h}}_m[k] = \sum_{l=1}^{L}\sum_{c=1}^{C_l} \frac{\sigma_{l,c,m}[k]}{\sqrt{LC_l}} \boldsymbol{a}_{N_{RX}}(\theta^{RX}_{l,c,m}, \phi^{RX}_{l,c,m}), \quad (1)$$

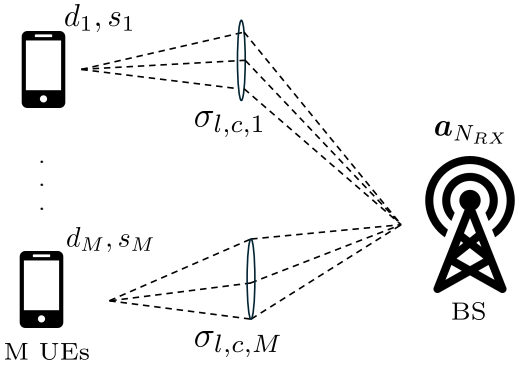

Fig. 1: Uplink mmWave SIMO ICC system.

where $\boldsymbol{a}_{N_{RX}}(\theta^{RX}_{l,c,m}, \phi^{RX}_{l,c,m})$ is the array response of the BS/AP receive antennas to the m-th UEs/EDs signal, θ_{RX} represents the elevation angle of arrival (AoA), ϕ_{RX} represents the azimuth AoA and $\sigma_{l,c,m}$ represents the time-varying small-scale fading coefficient.

Assuming that the BS/AP is equipped with a uniform planar array (UPA) with half-wavelength spacing, the array response can be expressed as

$$\boldsymbol{a}_N(\theta, \phi) = \boldsymbol{c}_{\sqrt{N_{RX}}}(\sin(\theta)\cos(\phi)) \otimes \boldsymbol{c}_{\sqrt{N_{RX}}}(\cos(\theta)), \quad (2)$$

where

$$\boldsymbol{c}_N(\nu) = [1, e^{j\pi\nu}, ...e^{j\pi(P-1)\nu}]. \quad (3)$$

For future convenience, a more tractable representation of the channel can be obtained by defining the channel matrix $\acute{\boldsymbol{H}}[k] \triangleq [\acute{\boldsymbol{h}}_1[k], \acute{\boldsymbol{h}}_2[k]...\acute{\boldsymbol{h}}_M[k]] \in \mathbb{C}^{N_{RX}\times M}$, and by extension, the array response matrix $\acute{\boldsymbol{A}}_{l,c} \triangleq [\boldsymbol{a}_{N_{RX}}(\theta^{RX}_{l,c,1}, \phi^{RX}_{l,c,1}), ...\boldsymbol{a}_{N_{RX}}(\theta^{RX}_{l,c,M}, \phi^{RX}_{l,c,M})] \in \mathbb{C}^{N_{RX}\times M}$.

The time dependency of the channel can be expressed in our small-scale fading coefficients. Given the initial $\sigma_{l,c,m}[0] \sim \mathcal{CN}(0, 1)$, future fading coefficients can be expressed using an auto-regressive (AR) model defined by

$$\sigma_{l,c,m}[k] = r\sigma_{l,c,m}[k-1] + \sqrt{1-r^2}\omega_{l,c,m}[k], \quad (4)$$

where $\omega_{l,c,m}[k] \sim \mathcal{CN}(0, 1)$ is a random time-varying factor and r is the correlation parameter between time-adjacent orthogonal frequency division multiplexing (OFDM) symbols.

The procedure for the estimation of r follows consecutively. The coherence time of the channel is given by

$$T_c = 0.432 \cdot \frac{v_c}{v}\frac{1}{f_c}, \quad (5)$$

where v_c, v and f_c are the speed of light, the relative velocity between transmitter and receiver and the carrier frequency respectively.

The symbol duration for a guard interval N_G times the total symbol size, an N_{DFT} DFT size and a sampling rate f_s, can be expressed as

$$T_s = N_{\text{DFT}} \cdot \frac{1 + N_G}{f_s}. \quad (6)$$

Leveraging the above, the discrete coherence time can be defined as $K_{\max} \triangleq \lfloor T_c/T_s \rfloor$. r can then be approximated by

$$r = \exp\left[\frac{\ln(0.5)}{K_{\max}}\right]. \quad (7)$$

B. Signal Model

Under the assumption of perfect synchronization between users, the received signal in one carrier at a discrete time k is given by

$$\begin{aligned}\boldsymbol{y}[k] &= \sum_{m=1}^{M} \boldsymbol{F}^{\mathsf{H}}_{RX}\acute{\boldsymbol{h}}_m[k]x_m[k] + \boldsymbol{w}[k] \\ &= \sum_{m=1}^{M} \boldsymbol{h}_m[k]x_m[k] + \boldsymbol{w}[k], \end{aligned} \quad (8)$$

where $\boldsymbol{F}_{RX} \in \mathbb{C}^{N_{RX}\times N}$ is the receive beamformer matrix, $\boldsymbol{h}_m \in \mathbb{C}^{N\times 1}$ is the effective (beam-domain) channel vector of the m-th UE/ED and $\boldsymbol{w} \sim \mathcal{CN}(0, N_0\boldsymbol{I}_N)$ is the circularly symmetric additive white Gaussian noise (AWGN).

To incorporate both communications and computing functionality, the transmit signal of each UEED is composed of a sum of a communication signal and a computing signal given by

$$x_m[k] = d_m[k] + \psi_m(s_m[k]), \tag{9}$$

where $d_m \in \mathcal{X}$ is a modulated communication symbol from discrete constellation $\mathcal{X}$ (i.e. quadrature phase shift keying (QPSK)) and $s_m \in \mathbb{R}$ is the m-th computing symbol, pre-processed by a function $\psi_m(\cdot)$.

A nomographic function (like our target function) is a function that can be expressed as

$$f(\boldsymbol{s}) = \phi\left(\sum_{m=1}^{M} \psi_m(s_m)\right). \tag{10}$$

For the sake of simplicity, the arithmetic sum is chosen as the target function, $i.e.$, $\phi(\cdot)$ and $\psi_m(\cdot), \forall m$, will be the identity map.

C. Beamforming

Under the assumption of perfect CSI, a popular beamforming scheme in MIMO communications uses the singular value decomposition (SVD) to diagonalize the channel. However, under the same assumption, due to the SIMO system architecture, data symbols cannot be combined before transmission and therefore, we employ a 'quasi-SVD' combiner. The construction of the receive beamformer will be the same as in the MIMO case, since the same receiver architecture is being used. At the transmitter, since we utilize single-antenna UEs/EDs, the beamformer is limited. Let us start with the fact that the time zero (known) channel can be decomposed as

$$\acute{\boldsymbol{H}}[0] = \boldsymbol{U}\boldsymbol{\Sigma}\boldsymbol{V}^{\mathsf{H}}. \tag{11}$$

The combiner can then be constructed as

$$\boldsymbol{F}_{RX} = [\boldsymbol{U}]_{:,1:N}, \tag{12}$$

where $N \leq N_{RX}$. If N is significantly larger than the number of clusters in our mmWave channel, we can fully exploit the channel's degrees of freedom.

This approach will not result in a fully diagonal effective channel, but instead, an upper-triangular channel matrix, which does not cause a significant hindrance to the performance of our detection scheme. The combiner is kept constant as the channel varies, so the effective channel can be formulated as

$$\boldsymbol{H}[k] = \boldsymbol{F}_{RX}^{\mathsf{H}}\acute{\boldsymbol{H}}[k] \in \mathbb{C}^{N\times M}. \tag{13}$$

For convenience, the effective channel can also be expressed as

$$\boldsymbol{H}[k] = \sum_{l=1}^{L}\sum_{c=1}^{C_l} \frac{1}{\sqrt{LC_l}} \boldsymbol{A}_{l,c}\boldsymbol{\sigma}_{l,c}[k], \tag{14}$$

where $\boldsymbol{A}_{l,c} = \boldsymbol{F}_{RX}^{\mathsf{H}}\acute{\boldsymbol{A}}_{l,c} \in \mathbb{C}^{N\times M}$ is the beam-domain array response matrix, and $\boldsymbol{\sigma}_{l,c} \triangleq \mathrm{diag}(\sigma_{l,c,1}[k], \dots \sigma_{l,c,M}[k])$ is the small-scale fading coefficient matrix of the c-th ray of the l-th cluster at time k.

III. Proposed Joint Communication, Computing and Channel Tracking Receiver

In this section, the framework for joint channel estimation/tracking and data detection proposed in [19] is augmented with the integration of AirComp, where we compute a target function with the computing symbols sent by each user as input. E_d represents the power allocated to the communications symbols and E_c is the power is allocated to the computing symbols such that $E_d + E_c = 1$. The communication symbols are modulated with QPSK and the computing symbols are normally distributed with zero mean; $s_k \sim \mathcal{N}(0, E_c)$. The soft replicas of the channel are defined as $\hat{h}_{nm,k}$, $\hat{\boldsymbol{h}}_{m,k}$, $\hat{\boldsymbol{H}}_k$ respectively for each channel coefficient, channel vector, and channel matrix respectively, with the respective MSEs being defined as $\hat{\psi}^h_{nm,k}$, $\hat{\boldsymbol{\Psi}}^h_{m,k}$ & $\hat{\boldsymbol{\Psi}}^h_k$.

The second-order statistics of the channel, assuming knowledge of a past channel, which are going to be useful in JCDE and CP are additionally calculated in [20], with their closed forms given by

$$\begin{aligned}\omega_{nm,k'} &= \mathbb{E}\left[|h_{nm}[k] - r^{k'}h_{nm}[k-k']|^2\right] \\ &= \frac{1-r^{2k'}}{L}\sum_{l=1}^{L}\sum_{c=1}^{C_l}\frac{|[\boldsymbol{A}_{l,c}]_{n,m}|^2}{C_l} = \frac{1-r^{2k'}}{L}\theta_{nm},\end{aligned} \tag{15a}$$

$$\begin{aligned}\boldsymbol{\Omega}_{m,k'} &= \mathbb{E}\left[(\boldsymbol{h}_m[k] - r^{k'}\boldsymbol{h}_m[k-k'])(\boldsymbol{h}_m[k] - r^{k'}\boldsymbol{h}_m[k-k'])^{\mathsf{H}}\right] \\ &= \frac{1-r^{2k'}}{L}\sum_{l=1}^{L}\sum_{c=1}^{C_l}\frac{[\boldsymbol{A}_{l,c}]_{:,m}[\boldsymbol{A}_{l,c}]_{:,m}^{\mathsf{H}}}{C_l},\end{aligned} \tag{15b}$$

$$\begin{aligned}\boldsymbol{\Omega}_{k'} &= \mathbb{E}_{\boldsymbol{H}[k']}\left[\boldsymbol{H}[k]\boldsymbol{H}[k]^{\mathsf{H}}|\boldsymbol{H}[k-k']\right] \\ &= \frac{1-r^{2k'}}{L}\sum_{l=1}^{L}\sum_{c=1}^{C_l}\frac{\boldsymbol{A}_{l,c}\boldsymbol{A}_{l,c}^{\mathsf{H}}}{C_l} = \frac{1-r^{2k'}}{L}\boldsymbol{\Theta},\end{aligned} \tag{15c}$$

where θ_{nm} and $\boldsymbol{\Theta}$ are the true variance of the channel coefficients and the covariance matrix of the channel, respectively.

For a considered set of time indices $\mathcal{K}$, the algorithm is performed in time windows $\mathcal{K}_\tau \subset \mathcal{K}$, which, due to an unchanging relative velocity assumption, can be constructed as having a constant length (determined by parameter W) and a constant number of new samples with respect to the previous window (determined by parameter D). The τ-th window can be defined as

$$\mathcal{K}_\tau = \{\, k \in \mathcal{K} \mid (\tau - D)W \leq k \leq \tau W - 1\}, \tag{16}$$

which consequently leads to $\tau_{max} = K/W + D - 1$ windows.

At each window, CP is carried out to provide better starting estimates, which are then utilized in the message passing algorithm for the data detection stage and then as a starting point for channel estimation.

A. Channel Prediction

The CP algorithm works by calculating the conditional expectation of the new channels given the known channels within any given window. Given knowledge of the channel at $k = 0$, the expectation can be expressed as

$$\mathbb{E}[\boldsymbol{H}[k]|\boldsymbol{H}[0]] = r^k\boldsymbol{H}[0], \tag{17}$$

with the the conditional variances being $\omega_{nm,k}$, $\mathbf{\Omega}_{m,k}$, and $\mathbf{\Omega}_k$ $\forall(n,m)$ for each channel coefficient, vector and matrix respectively.

In windows where $\tau \neq 1$, and the known channel is not available, the conditional expectation of the channel given the previously estimated channels that are still within the CP window is found. Note that the sub-optimality of the proposed JCDE algorithm results in the reliability of our channel estimates varying randomly with time. To alleviate this effect, the prior estimate that builds on the predictions is going to be the estimate k_τ with the minimum mean squared error (MSE) among the previously estimated channels in the current CP window, expressed as

$$k_\tau = \underset{k \in \mathcal{K}_\tau \backslash \mathcal{K}_\tau^+}{\operatorname{argmin}} \sum_{n=1}^{N} \sum_{m=1}^{M} \hat{\psi}^{\mathrm{h}}_{k,nm}, \tag{18}$$

where $\hat{\psi}_{nm,k}$ denotes the MSE of a channel coefficient JCDE estimate at time index k and $\mathcal{K}_\tau^+ = \mathcal{K}_\tau \backslash (\mathcal{K}_\tau \cap \mathcal{K}_{\tau-1})$ i.e. the set of new additions to the current time window.

After obtaining this MSE channel estimate, the predictions for the channel and the MSE of the channel estimates are updated as

$$\hat{\boldsymbol{H}}_k = \mathbb{E}\left[\boldsymbol{H}[k] | \hat{\boldsymbol{H}}_{k_\tau}\right] = r^{k-k_\tau} \hat{\boldsymbol{H}}_{k_\tau}, \tag{19a}$$

$$\hat{\psi}^h_{nm,k} = \omega_{nm,k-k_\tau} + r^{2(k-k_\tau)} \hat{\psi}^h_{nm,k_\tau}, \tag{19b}$$

$$\hat{\mathbf{\Psi}}^h_{m,k} = \mathbf{\Omega}_{m,k-k_\tau} + r^{2(k-k_\tau)} \hat{\mathbf{\Psi}}^h_{m,k_\tau}, \tag{19c}$$

$$\hat{\mathbf{\Psi}}^h_{k} = \mathbf{\Omega}_{k-k_\tau} + r^{2(k-k_\tau)} \hat{\mathbf{\Psi}}^h_{k_\tau}. \tag{19d}$$

Note that these equations are only used if $k > k_\tau$. If not, the estimates are not updated.

B. Data Detection

To initialize the algorithm, all communication symbol soft replicas $\hat{d}_{m,k}$ are set to 0 and their MSEs $\hat{\psi}^d_{m,k} = \mathbb{E}[|x_m[k] - \hat{x}_{m,k}|^2]$ are set to 1. During detection, the computing symbols are treated as effective noise, given by

$$\boldsymbol{y}[k] = \boldsymbol{H}[k]\boldsymbol{d}[k] + (\boldsymbol{H}[k]\boldsymbol{s}[k] + \boldsymbol{w}[k]) = \boldsymbol{H}[k]\boldsymbol{d}[k] + \tilde{\boldsymbol{w}}[k], \tag{20}$$

where $\boldsymbol{w} \sim \mathcal{CN}(0, \tilde{N}_0)$ is the effective noise with power $\tilde{N}_0 = N_0 + E_c$.

1) Factor Nodes: The soft interference cancellation (SIC) procedure is performed on the factor nodes, and can be expressed as

$$\tilde{\boldsymbol{y}}_{m,k} = \boldsymbol{y}[k] - \sum_{i \neq m}^{M} \hat{\boldsymbol{h}}_{k,i} \hat{d}_{i,k} = \hat{\boldsymbol{h}}_{m,k} d_m[k] \tag{21}$$

$$+ \underbrace{\tilde{\boldsymbol{h}}_{m,k} d_m[k] + \sum_{i \neq m}^{M} (\boldsymbol{h}_i[k] d_i[k] - \hat{\boldsymbol{h}}_{i,k} \hat{d}_{m,k}) + \tilde{\boldsymbol{z}}[k]}_{\text{Residual Interference and Noise } (\boldsymbol{\epsilon}^d_{k,m})}.$$

Using the vector Gaussian approximation (VGA), the probability density function (PDF) of $\boldsymbol{\epsilon}^d_{k,m}$ can be approximated by a Gaussian mixture model $p(\tilde{\boldsymbol{y}}_{m,k} | d_m[k])$ with mean vector $\hat{\boldsymbol{h}}_{m,k} d_m[k]$ and covariance matrix $\mathbf{\Xi}_{m,k}$, which is given by

$$\mathbf{\Xi}_{m,k} = \mathbb{E}[\boldsymbol{\epsilon}^d_{k,m}] \tag{22}$$

$$= \underbrace{\sum_{i=1}^{M} \hat{\boldsymbol{h}}_{i,k} \hat{\boldsymbol{h}}^{\mathsf{H}}_{i,k} \hat{\psi}^d_{ik} + \tilde{N}_0 \boldsymbol{I}_N + \hat{\mathbf{\Psi}}^h_k}_{\mathbf{\Xi}_k} - \hat{\boldsymbol{h}}_{i,k} \hat{\boldsymbol{h}}^{\mathsf{H}}_{i,k} \hat{\psi}^d_{mk},$$

2) Variable Nodes: Beliefs are combined across receive antennas in the variable nodes, leading to a joint belief. The PDF of these combined beliefs can be expressed by reformulating the vector distribution as a scalar, as

$$p(\tilde{\boldsymbol{y}}_{m,k} | d_m[k]) = \exp\left[\frac{|d_m[k] - \bar{d}_{m,k}|^2}{\bar{\psi}^d_{m,k}}\right], \tag{23}$$

with

$$\bar{d}_{m,k} = \frac{1}{\eta_{m,k}} \hat{\boldsymbol{h}}^{\mathsf{H}}_{m,k} \mathbf{\Xi}_m \tilde{\boldsymbol{y}}_{m,k}, \tag{24a}$$

$$\bar{\psi}^d_{m,k} = \frac{1 - \eta_{m,k} \hat{\psi}^d_{m,k}}{\eta_{m,k}}, \tag{24b}$$

where $\eta_{m,k} = \hat{\boldsymbol{h}}^{\mathsf{H}}_{m,k} \mathbf{\Xi}_m \hat{\boldsymbol{h}}_{m,k}$ is a term derived from the matrix inversion lemma, to eliminate the dependency of the used $\mathbf{\Xi}$ matrix on m.

3) Denoising and damping: The Bayes-optimal denoiser for QPSK symbols is used to obtain new estimates for the soft replicas, which are then damped to ease convergence. The denoiser is given by

$$\hat{d}'_{m,k} = c_d \left(\tanh\left(2c_d \tfrac{\Re(\bar{d}_{m,k})}{\bar{\psi}^d_{m,k}}\right) + j \tanh\left(2c_d \tfrac{\Im(\bar{d}_{m,k})}{\bar{\psi}^d_{m,k}}\right) \right), \tag{25a}$$

$$\hat{\psi}'^d_{m,k} = 1 - \left|\hat{d}_{m,k}\right|^2, \tag{25b}$$

where $c_d = \sqrt{E_d/2}$ is the real and imaginary part of the QPSK symbols transmitted.

Then, damping with a coefficient $0 \leq \beta \leq 1$ yields

$$\hat{d}_{m,k} = \beta \hat{d}'_{m,k} + (1-\beta) \hat{d}_{m,k}, \tag{26a}$$

$$\hat{\psi}'^d_{m,k} = \beta \hat{\psi}'^d_{m,k} + (1-\beta) \hat{\psi}^d_{m,k}. \tag{26b}$$

C. Channel Estimation

Channel coefficient beliefs have to be propagated in the time dimension for this phase, to make full use of our receive diversity. Due to this, a neighborhood is defined for the combining of beliefs in each time instance based on a window length parameter G, so as to avoid error propagation. At the τ-th iteration, the set around index k is defined as

$$\mathcal{S}_{k,\tau} = \left\{ s \in \breve{\mathcal{K}}_\tau \backslash \{k\} \middle| k - \frac{G}{2} \leq s \leq k + \frac{G}{2} \right\}, \tag{27}$$

where $\breve{\mathcal{K}}_\tau = \bigcup_{t=1}^{\tau} \mathcal{K}_t$.

1) Factor Nodes: The SIC is carried out as

$$\tilde{y}_{nm,k} = y_n[k] - \sum_{i \neq m}^{M} \hat{h}_{ni,k} \hat{d}_{i,k}. \tag{28}$$

Assuming that the effective noise component can be approximated via the scalar Gaussian approximation (SGA) to model errors due to AWGN, the computing signal, interference and channel aging, we can extract the following PDF for the aged SIC terms $r^{k-s} \tilde{y}_{nm,s}$ as

Algorithm 1 Proposed Joint Communication, Computing and Channel Estimation Algorithm

Input: $\boldsymbol{y}[k], \forall k$, $\boldsymbol{A}_{l,c} \forall l, c$, $\boldsymbol{H}[0]$, r, $\tilde{N}_0$, W, G, D, $t_{\max}$
Output: $\hat{\boldsymbol{d}}[k]$, $\hat{\boldsymbol{H}}[k]$, $\hat{f}(\boldsymbol{s}[k])$, $\forall k$

PREPROCESSING
Obtain $\mathcal{K}_\tau$ using (16), generate $\mathcal{K}_\tau^+$ and $\breve{\mathcal{K}}_\tau$
Obtain $\mathcal{S}_{k,\tau}$ using (27)
Initialize $\hat{d}_{m,k} = 0, \psi^d_{m,k} = 1$, $\forall (m,k)$
Obtain θ_{nm}, $\boldsymbol{\Theta}_m$, $\forall (n,m)$, using equations (15) respectively.
Obtain $\omega_{nm,k}$, $\boldsymbol{\Omega}_{m,k}$, $\boldsymbol{\Omega}_k$, $\forall (n,m,k)$ using (15) respectively.
CHANNEL PREDICTION
for $\tau = 1$ **to** τ_{max} **do**
  if $\tau = 1$, $\forall k \in \mathcal{K}_1$ **then**
    $\hat{\boldsymbol{H}}_k = r^k \boldsymbol{H}[0]$, $\hat{\boldsymbol{\Psi}}^{\mathsf{H}}_k = \boldsymbol{\Omega}_k$
    $\forall m$ $\hat{\boldsymbol{\Psi}}^h_{k,m} = \boldsymbol{\Omega}_{k,m}$
    $\forall (n,m)$ $\hat{\psi}^h_{nm,k} = \omega_{nm,k}$, $\forall$
  else
    $(\forall k \in \mathcal{K}_\tau, n, m)$ Obtain $\hat{\boldsymbol{H}}_k$, $\hat{\boldsymbol{\Psi}}^{\mathsf{H}}_k$, $\hat{\boldsymbol{\Psi}}^{\mathsf{H}}_{k,m}$, $\hat{\psi}^h_{nm,k}$ using equations (19).
  end if
  JCDE
  for t = 1 **to** $t_{\max}$, $\forall k \in \mathcal{K}_\tau$ **do**
    $\forall m$, obtain $\tilde{\boldsymbol{y}}_{m,k}$ using equation (21).
    Obtain $\boldsymbol{\Xi}_k$ using equation (22).
    $\forall m$, $\eta_{m,k} = \hat{\boldsymbol{h}}^{\mathsf{H}}_{m,k} \boldsymbol{\Xi}_m \hat{\boldsymbol{h}}_{m,k}$
    $\forall m$, obtain $\bar{d}_{m,k}$ *and* $\bar{\psi}^d_{m,k}$ using equations (24)
    $\forall m$, obtain $\hat{d}'_{m,k}$ and $\hat{\psi}'^d_{m,k}$ using equations (25)
    $\forall m$, update $\hat{d}_{m,k}$ and $\hat{\psi}^d_{m,k}$ using (26).
    $\forall (m,n)$, obtain $\tilde{y}_{nm,k}$ using equation (28)
    $\forall (m,n)$, obtain $\nu_{nm,k}$ using equation (31)
    $\forall (s \in \mathcal{S}_{k,\tau}, m, n)$, obtain $\nu_{nm,s\to k}$ using (30).
    $\forall (m,n)$
    if $t = t_{\max}$ **then**
      $\bar{\psi}^h_{nm,k} = \left(\sum_{s \in \mathcal{S}_{k,\tau} \cup \{k\}} \frac{|\hat{d}_{m,s}|^2}{\nu_{s\to k,nm}} \right)^{-1}$
      $\bar{h}_{nm,k} = \bar{\psi}^h_{nm,k} \sum_{s \in \mathcal{S}_{k,\tau} \cup \{k\}} \frac{\hat{d}^*_{nm,s} r^{k-s} \tilde{y}_{nm,s}}{\nu_{s\to k,nm}}$
    else
      $\forall (m,n)$, obtain $\bar{h}_{nm,k}$ and $\bar{\psi}^h_{nm,k}$ using equations (33).
    end if
    $\forall m$, obtain $\hat{\boldsymbol{h}}'_{m,k}$ and $\hat{\boldsymbol{\Psi}}'^h_{k,m}$ using equations (34).
    $\forall m$, update $\hat{\boldsymbol{h}}_{m,k}$ and $\hat{\boldsymbol{\Psi}}^h_{k,m}$ using (35)
  end for
end for
$\forall (m,k)$, $\hat{d}_m[k] = \operatorname{argmin}_{d \in \mathcal{X}} \left| d - \hat{d}_{m,k} \right|$
$\forall k$, $\hat{\boldsymbol{H}}[k] = \hat{\boldsymbol{H}}_k$
AIRCOMP
$\forall k \in \mathcal{K}$, Obtain $\boldsymbol{u}_k$ using equation (36).
$\forall k \in \mathcal{K}$, Obtain $\hat{f}(\boldsymbol{s}[k])$ using equation (38).

$$p(r^{k-s}\tilde{y}_{nm,s}|h_{nm}[k]) \propto \exp\left[\frac{|r^{k-s}\tilde{y}_{nm,s} - h_{nm}[k]\hat{d}_{mk}|^2}{\nu_{s\to k,nm}} \right], \tag{29}$$

where

$$\nu_{s\to k,nm} = \begin{cases} \omega_{s-k,nm} \left| \hat{d}_{m,s} \right|^2 + r^{2(k-s)} \nu_{s,nm} & k > s \in \mathcal{S}_{k,\tau}, \\ r^{2(k-s)} \left(\omega_{s-k,nm} \left| \hat{d}_{m,s} \right|^2 + \nu_{s,nm} \right) & k < s \in \mathcal{S}_{k,\tau}, \end{cases} \tag{30}$$

and $\nu_{s,nm}$ is defined as

$$\nu_{s,nm} = \sum_{i \neq m}^{M} \left\{ \left| \hat{h}_{ni,k} \right|^2 \hat{\psi}^d_{i,k} + \left(|\hat{d}_{m,i}|^2 + \hat{\psi}^d_{i,k} \right) \psi^h_{ni,k} \right\} + \theta_{nm} \hat{\psi}^d_{m,k} + \tilde{N}_0. \tag{31}$$

The dual formula for the interference-cancelled term's squared error (30) lends itself to the fact that we are propagating beliefs in the time dimension; beliefs propagated from the past and from the future have different statistical properties, as the error due to channel aging is scaled differently in the calculation of the effective noise component. Since the aforementioned error is zero-mean, however, this does not affect the SIC means. The θ_{nm} term is used as a substitute to the true channel gain $|h_{nm}[s]|^2$ at time instances.

2) Variable Nodes: At this stage, assuming the SGA, the effective noise PDFs of each belief are multiplied to get the extrinsic beliefs

$$\prod_{s \in \mathcal{S}_{k,\tau}} p(r^{k-s}\tilde{y}_{nm,s}|h_{nm}[k]) \propto \exp\left[\frac{h_{nm}[k] - \bar{h}_{nm,k}}{\bar{\psi}^h_{nm,k}} \right], \tag{32}$$

where

$$\bar{h}_{nm,k} = \bar{\psi}^h_{nm,k} \textstyle\sum_{s \in \mathcal{S}_{k,\tau}} \dfrac{\hat{d}^*_{nm,s} r^{k-s} \tilde{y}_{nm,s}}{\nu_{s\to k,nm}}, \tag{33a}$$

$$\bar{\psi}^h_{nm,k} = \left(\textstyle\sum_{s \in \mathcal{S}_{k,\tau}} \dfrac{|\hat{d}_{m,s}|^2}{\nu_{s\to k,nm}} \right)^{-1}. \tag{33b}$$

The extrinsic beliefs are generated, since their combining over the time dimension can alleviate error feedback from the SIC stage.

3) Denoising and damping: A Gaussian denoiser, obtained as an expectation of the channel vectors, conditioned on the extrinsic belief PDFs, is used for the soft replica updating for both the soft replicas and their MSE. First, let us define $\bar{\boldsymbol{h}}_{m,k} = [\bar{h}_{1m,k}, \dots \bar{h}_{Nm,k}]$, $\bar{\boldsymbol{\Psi}}^h_{k,m} = \operatorname{diag}[\bar{\psi}^h_{k,1m}, \dots \bar{\psi}^h_{k,Nm}]$ and the sum of the past and new covariance matrices $\boldsymbol{\Lambda}_{m,k} = \boldsymbol{\Omega}_{m,k} + \bar{\boldsymbol{\Psi}}^h_{k,m}$. Then, the new replicas can be generated as

$$\hat{\boldsymbol{h}}'_{m,k} = \boldsymbol{\Omega}_{m,k} \boldsymbol{\Lambda}^{-1}_{m,k} \bar{\boldsymbol{h}}_{m,k} + r^k \bar{\boldsymbol{\Psi}}^h_{k,m} \boldsymbol{\Lambda}^{-1}_{m,k} \boldsymbol{h}_m[k], \tag{34a}$$

$$\hat{\boldsymbol{\Psi}}'^h_{k,m} = \boldsymbol{\Omega}_{m,k} \boldsymbol{\Lambda}^{-1}_{m,k} \bar{\boldsymbol{\Psi}}^h_{k,m}. \tag{34b}$$

Finally, damping is performed with the same coefficient β, yielding

$$\hat{\boldsymbol{h}}'_{m,k} = \beta \hat{\boldsymbol{h}}'_{m,k} + (1-\beta) \hat{\boldsymbol{h}}_{m,k}, \tag{35a}$$

$$\hat{\boldsymbol{\Psi}}'^h_{k,m} = \beta \hat{\boldsymbol{\Psi}}'^h_{k,m} + (1-\beta) \hat{\boldsymbol{\Psi}}^h_{k,m}. \tag{35b}$$

D. AirComp

After successful detection for the communication symbols and channel estimation, we perform AirComp to obtain an estimate of the target function at time k using an MMSE combiner $\boldsymbol{u}_k \in \mathbb{C}^{N\times 1}$ on the channel residual as

$$\hat{f}(\boldsymbol{s}[k]) = \boldsymbol{u}_k^{\mathsf{H}}(\boldsymbol{y}[k] - \hat{\boldsymbol{H}}[k]\hat{\boldsymbol{d}}[k]). \tag{36}$$

The MMSE combiner is computed as the solution to the problem

$$\begin{aligned}\boldsymbol{u}_k &= \underset{\boldsymbol{u}_k\in\mathbb{C}^{N\times 1}}{\operatorname{argmin}} \left|\left|f(\boldsymbol{s}) - \hat{f}(\boldsymbol{s})\right|\right|_2^2 \\ &= \underset{\boldsymbol{u}_k\in\mathbb{C}^{N\times 1}}{\operatorname{argmin}} \left|\left|\mathbf{1}_M^{\mathsf{T}}\boldsymbol{s}[k] - \boldsymbol{u}_k^{\mathsf{H}}(\boldsymbol{y}[k] - \hat{\boldsymbol{H}}[k]\hat{\boldsymbol{d}}[k])\right|\right|_2^2.\end{aligned} \tag{37}$$

The combiner for time index k, which was computed without considering channel estimation error, is given by

$$\boldsymbol{u}_k = (\hat{\boldsymbol{H}}[k](\boldsymbol{\xi}_k + E_c\cdot\boldsymbol{I_M})\hat{\boldsymbol{H}}[k]^{\mathsf{H}} + N_0\boldsymbol{I}_N)^{-1}E_c\hat{\boldsymbol{H}}[k]\cdot\mathbf{1}_M, \tag{38}$$

where $\boldsymbol{\xi}_k \in \mathbb{C}^{M\times M}$ is the communication data estimation error covariance matrix, which is defined as $\mathrm{diag}[\psi_{1,k}^d, \dots \psi_{M,k}^d]$.

The algorithm is summarized in Algorithm 1. In addition to receive signals $\boldsymbol{y}[k], \forall k$, the algorithm takes as input $\boldsymbol{A}_{l,c}$, $\boldsymbol{H}[0]$, , r, $\tilde{N}_0$ and the design parameters (W, D, G), as well as the number of JCDE iterations $t_{\max}$. The output of the algorithm will be the detected communication symbols $\hat{\boldsymbol{d}}[k]$, the estimated channel $\hat{\boldsymbol{H}}[k]$ and the estimated output of the target function $\hat{f}(\boldsymbol{s}[k])$. The complexity of the JCDE phase of the algorithm is governed by matrix inversions (namely $\boldsymbol{\Xi}_k$s for the data detection & $\boldsymbol{\Lambda}_{k,m}$s). Both operations are performed M times across the users. Additionally, the window sizes D & W add to the complexity. The JCDE algorithm thus has a complexity of $\mathcal{O}(t_{max}N^3MWD)$. The complexity of the AirComp is then governed again by the inversion of a N by N matrix, yielding a complexity of $\mathcal{O}(N^3)$.

IV. Performance Analysis

A system with $N_{RX} = 16$ receive antennas, $P = 2$ receive antennas, $M = 2$ users, and $N = 8$ over $K = 128$ transmissions over time was simulated in MATLAB. The system was evaluated across different relative velocities (10-40 km/h) between transmitter and receiver, assuming the different transmitting UEs/EDs are moving at the same velocity. The system assumes an OFDM carrier frequency of $f_c = 60$ GHz with an OFDM sampling frequency of $f_s = 2.64$GHz. The DFT size was set to 512 and the guard interval to $1/4$-th of it [26]. The mmWave channel is modeled as having $L = 4$ clusters with $C_l = 15$ rays each. The algorithm parameters were set to $(W, D, G) = (8, 3, 6)$, $t_{\max} = 8$ and $\beta = 0.5$. The transmit power was set to $E_d = 0.99$ for communications and $E_c = 0.01$ for communications. No comparisons with benchmark schemes are included in the evaluation of our results, since we are presenting a state-of-the-art (SotA) integration of functionalities, which has not been discussed in previous work, and the isolated performance of every functionality is evaluated within the scheme.

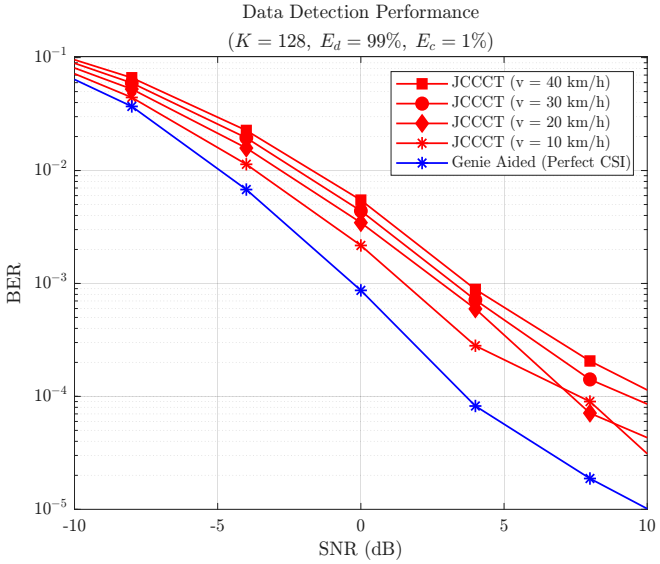

(a) BER performance of the system for different relative velocities.

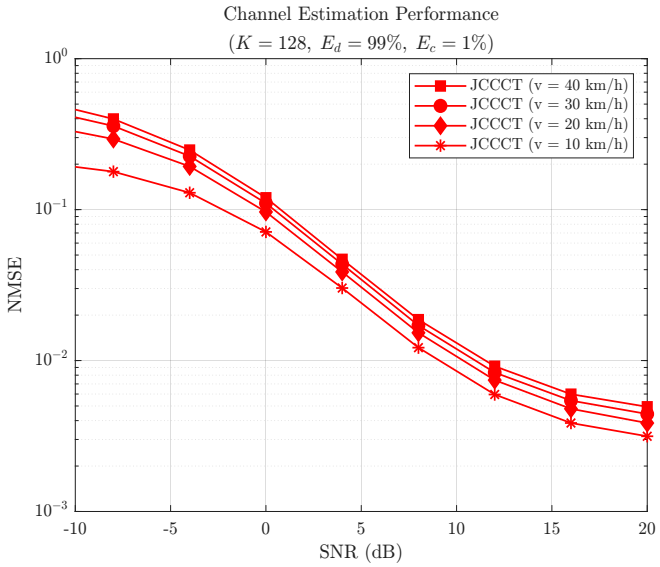

(b) Channel estimation performance for different relative velocities.

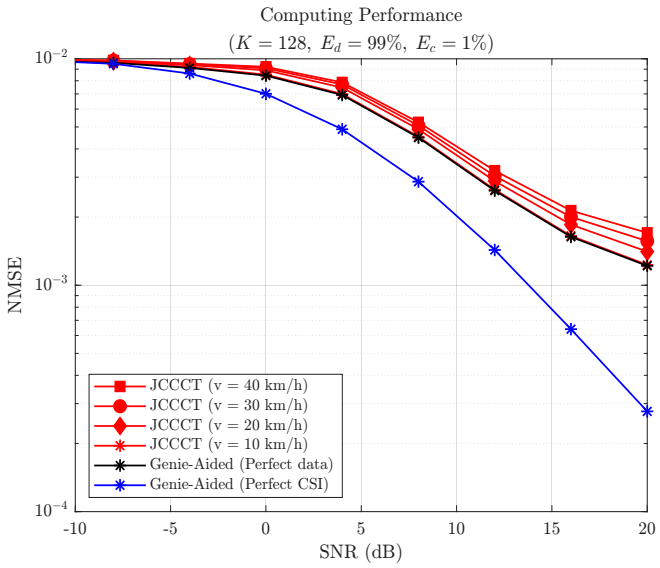

(c) AirComp performance compared to bounding references.

The BER was plotted for the communication symbols (Figure 2(a)), and the NMSE was plotted for the channel estimation (Figure 2(b)) and the AirComp (Figure 2(c)). The performance of the communications was also evaluated for a known channel to provide a bound.

The performance of AirComp was also evaluated for a known channel, as well as for known communication symbols (Figure 2(c)).

As can be observed from Figure 2(a), the proposed algorithm closely approaches the bound where perfect CSI is assumed, although the performance degrades with larger velocities due to the large Doppler shifts. A similar trend can be observed for the channel estimation performance as seen from Figure 2(b).

Finally, it can be observed from Figure 2(c) that the NMSE performance also matches the Genie-Aided case.

V. Conclusion

We proposed a system for ICC in time-varying mmWave channels, which also keeps track of the channel variations. The system uses a BiGaBP algorithm aided by a channel prediction mechanism to estimate communication symbols and the channel time variations, while the target function estimate is computed after detection using the channel residual. A beamforming scheme is also proposed for the multi-user mmWave communications based on the existing SVD technique for point-to-point MIMO communications to minimize interference in the channel, which eases detection. The computing signal only uses a small fraction of the transmit power, which means that the communication task is not penalized by the integration of computing. In contrast, the computing performance is also almost completely independent of the receiver's knowledge of the communication symbols.

References

[1] Z. Gao, Z. Wan, D. Zheng, S. Tan, C. Masouros, D. W. K. Ng, and S. Chen, "Integrated sensing and communication with mmwave massive mimo: A compressed sampling perspective," *IEEE Transactions on Wireless Communications*, vol. 22, no. 3, pp. 1745–1762, 2023.

[2] J. Choi, V. Va, N. Gonzalez-Prelcic, R. Daniels, C. R. Bhat, and R. W. Heath, "Millimeter-wave vehicular communication to support massive automotive sensing," *IEEE Communications Magazine*, vol. 54, no. 12, pp. 160–167, 2016.

[3] F. Liu, Y. Cui, C. Masouros, J. Xu, T. X. Han, Y. C. Eldar, and S. Buzzi, "Integrated sensing and communications: Toward dual-functional wireless networks for 6g and beyond," *IEEE Journal on Selected Areas in Communications*, vol. 40, no. 6, pp. 1728–1767, 2022.

[4] K. R. R. Ranasinghe, H. Seok Rou, G. Thadeu Freitas de Abreu, T. Takahashi, and K. Ito, "Joint channel, data, and radar parameter estimation for afdm systems in doubly-dispersive channels," *IEEE Transactions on Wireless Communications*, vol. 24, no. 2, pp. 1602–1619, 2025.

[5] B. Nazer and M. Gastpar, "Computation over multiple-access channels," *IEEE Transactions on Information Theory*, vol. 53, no. 10, pp. 3498–3516, 2007.

[6] K. Ando and G. T. F. de Abreu, "Low-complexity and high-performance combiners for over the air computing," in *2023 IEEE 9th International Workshop on Computational Advances in Multi-Sensor Adaptive Processing (CAMSAP)*, 2023, pp. 126–130.

[7] W. Fang, Y. Zou, H. Zhu, Y. Shi, and Y. Zhou, "Optimal receive beamforming for over-the-air computation," in *2021 IEEE 22nd International Workshop on Signal Processing Advances in Wireless Communications (SPAWC)*, 2021, pp. 61–65.

[8] T. Qin, W. Liu, B. Vucetic, and Y. Li, "Over-the-air computation via broadband channels," *IEEE Wireless Communications Letters*, vol. 10, no. 10, pp. 2150–2154, 2021.

[9] W. Liu, X. Zang, Y. Li, and B. Vucetic, "Over-the-air computation systems: Optimization, analysis and scaling laws," *IEEE Transactions on Wireless Communications*, vol. 19, no. 8, pp. 5488–5502, 2020.

[10] K. R. Rayan Ranasinghe, K. Ando, and G. T. Freitas de Abreu, "From theory to reality: A design framework for integrated communication and computing receivers," in *2025 International Conference on Computing, Networking and Communications (ICNC)*, 2025, pp. 865–870.

[11] S. Rangan, T. S. Rappaport, and E. Erkip, "Millimeter-wave cellular wireless networks: Potentials and challenges," *Proceedings of the IEEE*, vol. 102, no. 3, pp. 366–385, 2014.

[12] C.-X. Wang, J. Bian, J. Sun, W. Zhang, and M. Zhang, "A survey of 5g channel measurements and models," *IEEE Communications Surveys & Tutorials*, vol. 20, no. 4, pp. 3142–3168, 2018.

[13] A. Adhikary, J. Nam, J.-Y. Ahn, and G. Caire, "Joint spatial division and multiplexing—the large-scale array regime," *IEEE Transactions on Information Theory*, vol. 59, no. 10, pp. 6441–6463, 2013.

[14] A. Alkhateeb, O. El Ayach, G. Leus, and R. W. Heath, "Channel estimation and hybrid precoding for millimeter wave cellular systems," *IEEE Journal of Selected Topics in Signal Processing*, vol. 8, no. 5, pp. 831–846, 2014.

[15] Y. Liu, C.-X. Wang, J. Huang, J. Sun, and W. Zhang, "Novel 3-d nonstationary mmwave massive mimo channel models for 5g high-speed train wireless communications," *IEEE Transactions on Vehicular Technology*, vol. 68, no. 3, pp. 2077–2086, 2019.

[16] J. T. Parker, P. Schniter, and V. Cevher, "Bilinear generalized approximate message passing—part i: Derivation," *IEEE Transactions on Signal Processing*, vol. 62, no. 22, pp. 5839–5853, 2014.

[17] O. Shental, D. Bickson, P. H. Siegel, J. K. Wolf, and D. Dolev, "Gaussian belief propagation for solving systems of linear equations: Theory and application," 2008. [Online]. Available: https://arxiv.org/abs/0810.1119

[18] B. Li, N. Wu, and Y.-C. Wu, "Distributed inference with variational message passing in gaussian graphical models: Tradeoffs in message schedules and convergence conditions," *IEEE Transactions on Signal Processing*, vol. 72, pp. 2021–2035, 2024.

[19] T. Takahashi, S. Ibi, and S. Sampei, "Design of adaptively scaled belief in multi-dimensional signal detection for higher-order modulation," *IEEE Transactions on Communications*, vol. 67, no. 3, pp. 1986–2001, 2019.

[20] T. Takahashi, H. Iimori, K. Ishibashi, S. Ibi, and G. T. F. de Abreu, "Bayesian bilinear inference for joint channel tracking and data detection in millimeter-wave mimo systems," *IEEE Transactions on Wireless Communications*, vol. 23, no. 9, pp. 11 136–11 153, 2024.

[21] K. R. R. Ranasinghe, K. Ando, H. S. Rou, G. T. F. de Abreu, T. Takahashi, M. Di Renzo *et al.*, "A flexible design framework for integrated communication and computing receivers," *arXiv preprint arXiv:2506.05944*, 2025.

[22] Y. Tsai, L. Zheng, and X. Wang, "Millimeter-wave beamformed full-dimensional mimo channel estimation based on atomic norm minimization," *IEEE Transactions on Communications*, vol. 66, no. 12, pp. 6150–6163, 2018.

[23] Z. Xiao, X.-G. Xia, D. Jin, and N. Ge, "Iterative eigenvalue decomposition and multipath-grouping tx/rx joint beamformings for millimeter-wave communications," *IEEE Transactions on Wireless Communications*, vol. 14, no. 3, pp. 1595–1607, 2015.

[24] R. W. Heath, N. González-Prelcic, S. Rangan, W. Roh, and A. M. Sayeed, "An overview of signal processing techniques for millimeter wave mimo systems," *IEEE Journal of Selected Topics in Signal Processing*, vol. 10, no. 3, pp. 436–453, 2016.

[25] R.-A. Stoica, H. Iimori, G. T. Freitas de Abreu, and K. Ishibashi, "Frame theory and fractional programming for sparse recovery-based mmwave channel estimation," *IEEE Access*, vol. 7, pp. 150 757–150 774, 2019.

[26] C. Cordeiro, D. Akhmetov, and M. Park, "Ieee 802.11ad: introduction and performance evaluation of the first multi-gbps wifi technology," in *Proceedings of the 2010 ACM International Workshop on MmWave Communications: From Circuits to Networks*, ser. mmCom '10, 2010, p. 3–8.